Metallomics

Accepted Manuscript

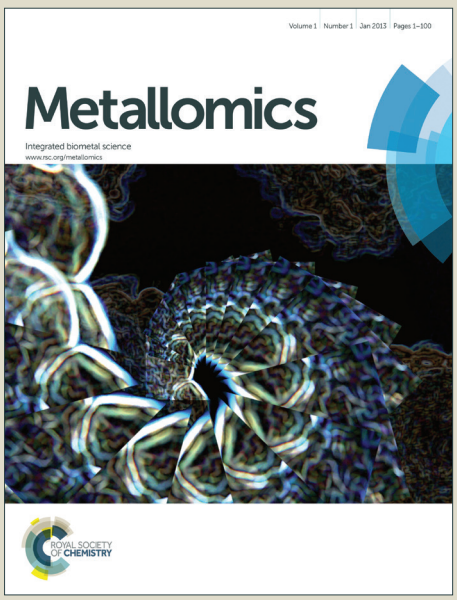

ROYAL SOCIETY OF CHEMISTRY

www.rsc.org/metallomics

Colchicine induced intraneuronal free zinc accumulation and dentate granule cell degeneration

Bo Young Choi[1, #], Bo Eun Lee[1,#], Jin Hee Kim[1], Hyun Jung Kim[1], Min Sohn[1], Hong Ki Song[3], Tae Nyoung Chung[4], Sang Won Suh[1, *]

[1] Department of Physiology, College of Medicine, Hallym University, Chuncheon, Korea, [2] Inha University, Department of Nursing, Incheon, Korea, [3] Department of Neurology, Institute of Epilepsy Research, College of Medicine, Hallym University, Chuncheon, Korea,[4] Department of Emergency Medicine, CHA University School of Medicine, Bundang, Korea

Corresponding Author [*] :

Sang Won Suh, MD, PhD Tel: (82-10) 8573-6364

1-Okcheon Dong, Dept. of Physiology, Fax: (82) 33-248-2580

Hallym University, College of Medicine. E-mail: swsuh@hallym.ac.kr

Chuncheon, Korea 200-702

[#] Equally contributed.

ABSTRACT

Colchicine has been discovered to inhibit many inflammatory processes such as gout, familiar Mediterran fever, pericarditis and Behcet disease. Other than these beneficial anti-inflammatory effects, colchicine blocks microtubule-assisted axonal transport, which results in the selective loss of dentate granule cells of the hippocampus. The mechanism of the colchicine induced dentate granule cell death and depletion of mossy fiber terminals still remain unclear. In the present study we hypothesized that colchicine-induced granule cell death may be caused by accumulation of labile intracellular zinc. 10 ug/kg of colchicine was injected into the adult rat hippocampus and then brain sections were evaluated at 1 day or 1 week later. Neuronal cell death was evaluated by H&E staining or Fluoro Jade-B. Zinc accumulation and vesicular zinc were detected by N-(6-methoxy-8-quinolyl)-para-toluene sulfonamide (TSQ) staining. To test whether an extracellular zinc chelator can prevent this process, CaEDTA was injected into the hippocampus over a 5-minute period with colchicine. To test whether other microtubule toxins also produce similar effect as colchicine, vincristine was injected into the hippocampus. The present study found that colchicine injection induced intracellular zinc accumulation in the dentate granule cells and depleted vesicular zinc from mossy fiber terminals. Injection of a zinc chelator, CaEDTA, did not block the zinc accumulation and neuronal death. Vincristine also produced intracellular zinc accumulation and neuronal death. These results suggest that colchicine-induced dentate granule cell death is caused by block of axonal zinc flow and accumulation of intracellular labile zinc.

Key words: zinc, colchicine, vincristine, TSQ, dentate granule cell, CaEDTA

INTRODUCTION

Colchicine has been discovered to inhibit many inflammatory processes. It is a toxic natural product, originally extracted from plants of the genus Colchium (autumn crocus). Colchicine is a classical drug for treating gout [1-3]. In addition to treatment of gout, colchicine has been used to treat familiar Mediterran fever [4], pericarditis [5, 6], and Behcet disease [7]. Colchicine inhibits microtuble polymerization by binding to tubulin, one of the main constituents of microtubules. Tubulin is essential to cellular mitosis, and therefore colchicine effectively acts as a "mitotic poison". Since one of the characteristics of cancer cells is increased rate of mitosis, cancer cells are more vulnerable to colchicine toxicity than are normal cells. However, the therapeutic value of colchicine against cancer is limited by its toxicity against normal cells. Long-term treatment of colchicine is absolutely contraindicated in patients with renal failure since substantial amount of colchicine is excreted unchanged by the kidneys. Therefore cumulative toxicity is possible in this clinical setting. The intracerebroventricular injection of colchicine appears to exert a direct toxic effect on cholinergic neurons and/or nerve terminals that results in cognitive impairments [8]. Hippocampal infusion of colchicine resembles those seen in Alzheimer's disease such as cognitive impairment and choline acetyltransferase (ChAT) activity reduction [9].

The migration of proteins within the neuron has demonstrated both a rapid (100-500 mm/day) and a slow (1-26 mm/day) mode of axonal transport from the neuronal bodies to the nerve terminals [10]. Colchicine blocks microtubule-assisted axonal transport mechanism and blocks protein turnover between body and terminals. Thus, injection of 10 ug/kg of colchicine into the hippocampus of mature rats results in degeneration of

dentate granule cell [11, 12]. Colchicine resulted in the selective loss of dentate granule cells, while sparing the pyramidal cells of the hippocampus. The destructive effects of colchicine appear as soon as 12 hr after the injection and lead to the disappearance of the granule cells over a period of days. At long post-injection survival intervals the disappearance of the granule cells is accompanied by elimination of their terminal projections, the mossy fibers. The mechanism of the colchicine induced dentate granule cell and depletion of mossy fibers, however, is still unknown.

A substantial amount of chelatable zinc is present in axonal boutons throughout the mammalian central nervous system. Loosely bound or labile zinc is present in a subset of glutamatergic axon terminals throughout the mammalian forebrain, especially in the synaptic terminals of dentate granule cells of hippocampus [13, 14]. The chelatable zinc is localized in presynaptic terminal vesicles [15] and is released into the extracellular space during neuronal depolarization [16, 17]. This zinc release has been demonstrated to contribute to neuronal death during several brain insults, such as prolonged seizure activity [18-20], ischemia [21, 22], traumatic brain injury [23, 24] and hypoglycemia [25, 26]. Blockade of zinc translocation with extracellular zinc chelator CaEDTA markedly reduced selective neuronal death following transient cerebral ischemia [21], traumatic brain injury [23] and hypoglycemia [25]. These findings suggest that zinc neurotoxicity may indeed be an underlying mechanism of selective neuronal death following the above brain insults. The mechanism by which zinc causes neuronal death has not been firmly established, and may be multifactorial [27-29]. Several lines of evidence suggest that zinc accumulation in neurons can induce oxidative stress, DNA damage, activation of the poly(ADP-ribose)

polymerase-1 cell death pathway [30-34] and NADPH oxidase activation [34, 35]. However, neuronal zinc deficiency can also induce oxidative stress and later cause apoptosis [36, 37].

Until now, the mechanisms of zinc uptake into the cell body and transport to the synaptic terminal vesicles were unknown. If zinc is incorporated in the soma and transported to the synaptic terminals, these processes should be blocked by microtubule transporter blocker colchicine. Furthermore, if the zinc uptake process into neurons is unchanged after colchicine treatment, zinc accumulation in the cell body would likely continue to build up until neuronal degeneration. For these reasons, neurons have high rates of zinc uptake and axonal zinc transport properties would be especially susceptible to microtubule transport inhibitors such as colchicine or vincristine.

The present study hypothesized that colchicine-induced selective granule cell degeneration may be caused by intracellular labile zinc accumulation. Here we found four lines of evidence: (i) colchicine induced intracellular zinc accumulation and dentate granule cells death; (ii) colchicine induced vesicular zinc depletion from the mossy fiber terminals; (iii) extracellular zinc chelator did not prevent these phenomena; and (iv) vincristine also produced same zinc accumulation and neuronal dentate granule cell death. All four phenomena were observed, supporting our hypothesis that colchicine-induced dentate granule cell death is caused by intracellular labile zinc accumulation.

MATERIALS AND METHODS

Ethics Statement

Animal studies were approved by the Committee on Animal Use for Research and Education at Hallym University (protocol # Hallym 2013-129), in compliance with NIH guidelines. Animal sacrifice was performed under isoflurane anesthesia and all efforts were made to minimize suffering.

Animal handling

Male Sprague-Dawley rats were used in this study (250 - 300 g, DBL Co). The animals were housed in a temperature- and humidity-controlled environment (22±2 °C, 55±5% and a 12 hr light: 12 hr dark cycle), supplied with Purina diet (Purina, Gyeonggi, Korea) and water *ad libitum*.

Combined Colchicine/ zinc chelator intrahippocampal injection

Intrahippocampal colchicine injection (10 ug/kg/ul, n=7) and saline injection (Vehicle, n=7) was performed under isoflurane anesthesia using stereotaxic apparatus (David-Kopf). A 1.0 mm burr hole was made on skull at 4 mm lateral from the midline, 4.5 mm caudal to bregma, and the syringe needle tip was lowered 3.5 mm below the cortical surface. CaEDTA was prepared as 1 mM solutions in physiological saline and brought to neutral pH with NaOH. Colchicine (10 ug/kg/ul) or colchicine with 1 mM CaEDTA was injected into the hippocampus over a 5-minute period. Another mitotic inhibitor, vincristine (10 ug/kg/ul, Vinc, n=4), also was injected into hippocampus to compare with colchicine.

Zinc staining

Histological evaluation was performed 24 and 48 hours after colchicine or 24 hours after vincristine injection. The N-(6-methoxy-8-quinolyl)-para-toluenesulfonamide (TSQ) histochemical method was used as previously described [38, 39]. For TSQ assay, rats were euthanized with a urethane (1.5 g/kg, i.p.) and the brains were quickly removed then frozen in powered dry ice. The frozen, unfixed brains were coronally sectioned at 20 μm thickness in a -19 ^{o}C cryostat, then thawed on to gelatin-coated slides and dried by gentle air. The sections were immersed in a solution of 4.5 μM TSQ (Molecular Probes, Eugene, OR) in 140 mM sodium barbital and 140 mM sodium acetate buffer (pH 10.5-11) for 60 seconds, and then rinsed for 60 seconds in 0.9 % saline. TSQ binding was imaged with a fluorescence microscope (Zeiss upright microscope, epi-illuminated with 360 nm UV light) and photographed through a 500 long-pass filter using a Hamamatsu 3 CCD cooled digital color camera C4742-95 (Hamamatsu Co., Bridgewater, NJ) with Openlab 3 imaging program (Improvision, Boston, MA). For signal quantification, the mean fluorescence intensity within the designated regions of interest (mossy fiber terminal area) was measured with Adobe Photoshop (6.0). Background correction was performed by subtracting the mean intensity of 1 mm^2 molecular layer of the dentate gyrus. Five sections obtained from an individual brain were used for quantification and these results were averaged for each “n”.

Assessment of neuronal death by H&E staining or Fluoro-Jade B (FJB)

Rats were euthanized 7 days after colchicine injection by 5 % isoflurane anesthesias. Coronal 30 μm frozen sections were prepared, fixed in 70% ethanol, and stained with haematoxylin and eosin (H&E) [23]. Five coronal sections were collected from

each animal, spaced 80 μm apart, starting 4.0 mm posterior to Bregma. A 10X microscopic field was centered on the structure of interest, and the total number of eosinophilic neurons in the structure of interest was recorded by an observer blinded to the experimental groups. Cell counts were made on both left and right hemispheres. Data from each animal were expressed as the mean number of eosinophilic neurons per structure of interest. To evaluate degenerating neurons, brain sections were also stained with Fluoro-Jade B (FJB) [40-42]. Degenerating neurons were detected by illumination under an epifluorescence microscope with a 450 to 490 nm excitation filter and a 515 nm emission filter.

Autometallography (AMG) vesicular zinc staining

For the permanent $ZnSe^{AMG}$ zinc staining, colchicine or vehicle injected rats were anesthetized with isoflurane after 7 days. Animals were intraperitoneally injected sodium selenide (10 mg/kg) dissolved in PBS. Ninety minutes later the animals were transcardially perfused with 0.1% NaS in 3% glutaraldehyde in 0.1 M phosphate buffer for 10 min. The brains were allowed to postfix in the 3% glutaraldehyde for 1 h, placed in a solution of 30% sucrose until they sank to the bottom of the vial, and were frozen with CO_2 gas. The brains were cut, 30 μm thick, and placed on glass slides cleaned in a 10% Farmer's solution [43, 44]. The sections were dried for 15 min, fixed in 90% ethanol, rehydrated and coated with 0.5% gelatin. The freshly prepared autometallographic (AMG) developer was poured into Farmer rinsed jars containing the slides, which were placed in a 26 °C water bath. Under this temperature 30-μm cryostat sections were developed for 60 min. The AMG development process was stopped by replacing the developer with 5%

sodium thiosulphate solution. After development, the slides were first rinsed in running tap water at 40 °C for 20 min in order to remove the gelatin coat, and then dipped twice in distilled water. After the rinse the sections were finally counterstained with toluidine blue. After rinsing and dehydration the sections were mounted with DePex mounting medium (BDH Laboratory Supplies, Poole, UK).

Vesicular zinc density after AMG staining

After AMG staining, brain sections were mounted in the microscope, trans-illuminated with a fixed intensity of white light (tungsten), and individual images were captured by a CCD camera, digitized, and stored. Ten sections that were obtained from an individual brain were used for quantification. Images were captured from each section, including the hilus of the dentate gyrus (DG) of the hippocampus. The measured zones were digitized as follows: reference: a square of stratum lacunosum-moleculare just overlying the middle of the blade of the dentate gyrus; hilus, the same square moved to the hilar confluence. Optical Density (OD) was calculated conventionally (OD = (log 10[incident light/transmitted light])), with “incident light” taken as the intensity of light transmitted through the zinc-free reference zone (in lacunosum-moleculare away from the lateral perforant path innervation), and “transmitted light” taken as the raw intensity reading for individual samples [45].

ZnT3-immunocytochemistry ($ZnT3^{ICC}$)

Seven days after the colchicine injection, seven rats from each colchicine or vehicle treated group were perfused with 4% paraformaldehyde in 0.1 M PBS (phosphate

buffered saline, pH 7.4). The brains were obtained and post-fixed using the same fixative (4 h, 4°C). The brains were placed in a vial filled with 30% sucrose in 0.1 M PBS (2 days, 4°C). An affinity-purified rabbit antibody specific for ZnT3 (provided by R.D. Palmiter) was used for immunocytochemical localization in the rat hippocampus. The immunolabeling procedures were performed in accordance with a routine avidin-biotin complex (ABC) (ABC kit; DAKO) method. The sections were incubated for 1 day at 4°C in ZnT3 antiserum, diluted 1:100 in TBS (Tris Buffered Saline) containing 3% goat serum, and 1% BSA and Triton. Following rinses for 45 min in TBS containing Triton, the sections were incubated in biotinylated goat anti-rabbit IgG (diluted 1:200) for 1 h at room temperature (22°C), rinsed for 30 min in TBS and then incubated in ABC, diluted 1:100 in 1% BSA and TBS for 1 h at room temperature. Sections were rinsed in TB (pH 7.6) and incubated for 15 min in 0.025% 3,3'-diaminobenzidine (DAB) with 0.0033% H_2O_2. Stained sections were rinsed in TBS followed by alcohol dehydration and xylene clearance.

Statistical analysis

Data were presented as means ± SEM. Statistical significance was assessed by analysis of variance (ANOVA) followed by the Student-Newman-Keuls post hoc test comparing all groups.

RESULTS

Colchicine induces intracellular zinc accumulation in dentate granule cells

To test whether colchicine-induced dentate granule cell death is caused by intracellular zinc accumulation, rats were sacrificed at 24 hours after colchicine injection. Vesicular zinc is detected by TSQ zinc staining. As shown in previous studies histochemically reactive zinc is present in the hippocampal mossy fiber region[14, 46]. In the vehicle treated rats, TSQ positive staining intensity is higher than dentate granule cell layer, where granule cells appear as dark "holes" surrounded by some scattered vesicular zinc (Fig. 1A). Hippocampal sections harvested 24 hours after the colchicine injection showed an intense fluorescence signal in the cell bodies of dentate granule cells (Fig. 1B) indicative of labile zinc accumulation in these cells. This accumulation started as early as 12 hr post-injection (data not shown). Neuronal death was evaluated by standard hematoxylin / eosin staining of brains harvested 24 hours after the colchicine injection, at which time degenerating (dead) dentate granule neurons are pyknotic and eosinophilic (Figs. 1C,D).

Mossy fiber vesicular zinc is depleted by colchicine injection

Vesicular zinc depletion was also evaluated by TSQ fluorescent zinc staining at 24 and 48 hours after colchicine injection. TSQ fluorescent intensity from the injured side was depressed by 34.0 % at 24 hours and 65.9 % at 48 hours after colchicine injection compared to vehicle treated control intensity (Figs. 2A,B).

Zinc depletion after colchicine injection is detected by autometallography (AMG)

As shown previously [23, 46, 47], the AMG patterns were in particular dense in the hilar area of hippocampus. Dense labeled AMG particle was present in the mossy fiber area than in the dentate granule cell layer. The intensity of vesicular zinc measured from hilar area 7 days after the colchicine injection showed significant depletion in the mossy fiber area (Figs. 3A,B) as seen in previous study [11]. The intensity of zinc from the injured side was depressed 71.76 % from vehicle treated control intensity (Fig. 3C).

ZnT3 immunostaining is decreased by colchicine injection

The ZnT3^{Icc} stained sections revealed a characteristic pattern in the mossy fiber area of hippocampus (Fig. 3D). More ZnT3 labeling presented in the mossy fiber area than in the dentate granule cell layer. The density of ZnT3-immunoreactivities was apparently decreased in the colchicine-injected ipsilateral hippocampus at 7 days after the colchicine injection.

Zinc chelation by CaEDTA showed no prevention of intracellular zinc accumulation in the dentate granule cells after colchicine injection

To test whether an extracellular zinc chelator can prevent intracellular zinc accumulation in dentate granule cells, rats were injected with colchicine with CaEDTA. Hippocampal sections harvested 24 hours after the colchicine injection showed several TSQ (+) neurons in the dentate gyrus while vehicle treated sections showed no TSQ (+) neurons. Zinc chelator CaEDTA showed no differences in number of TSQ (+) neurons (Figs. 4A,B). Dentate granule cell degeneration was evaluated by Fluoro-Jade B (FJB).

Vehicle-treated, sham operated hippocampal sections showed no FJB (+) neurons. Colchicine injection induced several FJB (+) neurons in the hippocampus, which is similar with H&E staining pattern. Colchicine-induced neurodegeneration was not attenuated by CaEDTA injection (Figs. 4C,D). These results represent colchicine-induced intracellular free zinc increase may not come from extracellular but come from intracellular components.

Vincristine induces zinc accumulation and dentate granule cell death

To test whether a different mitotic inhibitor also can produce a similar pattern of zinc accumulation and neuronal death in the dentate granule cell, rats were injected with vincristine intrahippocampally and sacrificed 24 hours later. Vincristine injection also produced intracellular zinc accumulation in dentate granule cells (Fig. 5A). Vincristine also induced neuronal death (eosinophilic neurons) as seen in colchicine-injected hippocampus (Figs. 5B,C).

Discussion

Using colchicine-induced dentate granule cell death model, the present study demonstrates: (i) toxic concentrations of intracellular zinc accumulation in the dentate granule cell of hippocampus; (ii) depletion of vesicular zinc from the mossy fiber pre-synaptic terminals; (iii) no reduction of colchicine-induced zinc accumulation and neuronal death by zinc chelator; and (iv) intracellular zinc accumulation and dentate granule cell degeneration by vincristine. Taken together, these results suggest a new neuronal death

mechanism that arises by blockade of axonal zinc transport and subsequent intracellular labile zinc accumulation as intermediary steps linking colchicine induced dentate granule cell death.

Zinc is the second most abundant transition metal (after iron) in the brain. Zinc is an essential element for DNA synthesis, development, immune function, and other important physiological processes. Most zinc in the soma is bound by proteins but chelatable zinc is localized in the synaptic vesicle of axon terminals. Anterograde and retrograde zinc transport between cell body and axon terminal is important to maintain neuronal function [48, 49]. Axonal transport of cytoplasmic material between neuronal processes and cell body is essential to neuronal physiology and survival. Abnormal axonal transport has been shown to occur in several central nervous system disorders such as amyotrophic lateral sclerosis (ALS) [50]. Also, a recent study suggested that intra-neuronal zinc dyshomeostasis and abnormal microtubule dynamics may be related to Alzheimer's disease associated neurodegeneration and cognitive decline[51].

The loss of zinc from mossy fiber terminals, coupled with the accumulation of zinc in their original cell bodies, suggests that colchicine blocks axonal transport of zinc between the two sites. Since colchicine would be expected to block microtubule-assisted axonal transport mechanisms, colchicine may block anterograde transport and force the accumulation of labile zinc in the soma. Axonal zinc transport between soma and synaptic terminal has been demonstrated directly in the brain [52, 53]. Wang and Dahalstrom demonstrated that a rapid bidirectional accumulation of AMG granules occurred in axons of crushed sciatic nerves. Also ZnT3 immunoreactivity was found to accumulate rapidly in anterograde as well as retrograde direction [54]. Thus, above and our present study

suggest that impaired axonal transport causes intracellular zinc accumulation in the neuron soma (Fig. 6). To rule out a possibility that extracellular originated zinc influx may cause this intracellular zinc accumulation we used an extracellular zinc chelator, CaEDTA. The present study found that intra-neuronal zinc accumulation after colchicine injection is not blocked by CaEDTA. This result suggests that the colchicine-induced zinc accumulation observed in dentate granule cells is a result of blocking axonal zinc transport from the soma to the synaptic terminals. Thus, extracellular cell-impermeable zinc chelator has no effect to prevent intracellular zinc accumulation and subsequent neuronal death.

According to Goldschmidt and Steward [11], hippocampal granule cells and mossy fibers degenerate slowly after intrahippocampal colchicine injection. Because these regions contain high concentrations of zinc in their presynaptic terminals it is likely that zinc containing vesicles were depleted after granule cell degeneration. We evaluated these phenomena by light microscope after AMG zinc staining. Here we found that mossy fiber zinc is almost completely depleted from the presynaptic terminals at 7 days later. We found that zinc transporter 3 (ZnT3) in mossy fiber is also almost completely disappeared from the presynaptic terminals at this time. Aniksztejn et al. previously demonstrated that colchicine-induced dentate granule cell death blocked depolarization-induced vesicular zinc release from the hippocampus, which is consistent with depletion of vesicular zinc after dentate granule cell death [55].

Many brain regions with high vesicular zinc concentrations exhibit high vulnerability to colchicine injection, but this is not universally the case. Some brain regions with very high zinc content, such as CA3 hippocampus, are not correspondingly sensitive to

colchicine [56]. Thus zinc cannot be the sole determinant of colchicine-dependent dentate granule neuron death, but may be a contributing factor in regions where synaptic terminal zinc concentrations and axonal transport rates are high.

Taken together, the present study confirms our hypothesis that inhibition of axonal transport by colchicine may induce intracellular free zinc accumulation and dentate granule cell degeneration.

ACKNOWLEDGEMENTS

This work was supported by the National Research Foundation of Korea (NRF) grant funded by the Korea government (MEST) (2012R1A2A2A01040132) and by a grant from the Hallym University Specialization Fund (HRF-S-51).

Conflict of interest

The authors declare no conflict of interest.

Figure legends

Figure 1. Colchicine-induced intracellular zinc accumulation and neuronal death in the dentate granule cell layer of hippocampus.

Fluorescent photomicrographs show TSQ zinc staining in the hippocampal dentate granule cells layer at 24 hours after colchicine injection. The dark holes in the sham operated vehicle-injected hippocampal sections represent the normal appearance of neuronal cell bodies, and the bright white fluorescence in the cell bodies from the colchicine-injected hippocampal sections indicates abnormal zinc accumulation in the dentate granule cells. **(A)** TSQ fluorescent image represents vehicle treated rat's hippocampal dentate granule cell layer. MF: Mossy fiber. DG: Dentate gyrus. **(B)** Fluorescence image represents abnormal intracellular zinc accumulation in the hippocampal dentate granule cells. White colored neurons in the DG area are TSQ positive neurons. Light microscopic images show haematoxylin and eosin (H&E) stained hippocampal sections. **(C)** H&E stained dentate granule cell layer. Purple colored neurons represent normal, un-injured neurons in the hippocampus. **(D)** Colchicine injection produces eosinophilic neurons in the dentate granule cell layer. Scale bar in (D) represents 100 μm.

Figure 2. TSQ fluorescence imaging of hippocampal zinc depletion after colchicine injection.

TSQ fluorescent microscopy shows vesicular zinc depletion in the hippocampus at 24

and 48 hours after the colchicine injection. **(A)** Black and white fluorescent image shows sham operated and colchicine injected hippocampus after TSQ staining. Zinc ions heavily stained in mossy fiber of hippocampal hilus in sham operated rats. Colchicine injection decreases TSQ fluorescent intensity at 24 and 48 hours later. Scale bar represents 100 μm. **(B)** Bar graph depict the optical density of zinc in hippocampal mossy fiber area. Optical density was measured from vehicle- and colchicine-injected rats at 24 and 48 hours later. Values are presented as means+S.E. Asterisk (*) denotes difference from vehicle-injected rats at $P < 0.05$.

Figure 3. Colchicine-induced vesicular zinc and ZnT3 depletion.

AMG light microscopy shows vesicular zinc depletion in the hippocampus 1 week after the colchicine injection. **(A)** Image shows perfusion-fixed AMG stained vehicle treated hippocampus. Zinc ions heavily stained in mossy fiber of hippocampal hilus. Less dense zinc staining is seen in stratum radiatum of the CA1. **(B)** AMG stained sections show 1 week after colchicine-injected hippocampus. Zinc staining intensity significantly decreased in mossy fibers of the hippocampal hilus. Scale bar represents 500 μm. **(C)** Bar graph depicts the optical density of zinc in hippocampal hilus area. Optical density was measured from vehicle- and colchicine-injected rats at 1 week later. Values are presented as means+S.E. Asterisk (*) denotes difference from vehicle-injected rats at $P < 0.05$. **(D)** Images show ZnT3 immunohistochemistry 1 week after colchicine-injected hippocampus. ZnT3 staining substantially decreased in mossy fibers of the hippocampus. Scale bar represents 500 μm.

Figure 4. Zinc chelator, CaEDTA, shows no prevention of colchicine-induced intracellular zinc accumulation and dentate granule cell death.

Fluorescent photomicrographs show TSQ stained hippocampal dentate granule cells layer **(A,B,C)**. **(A)** The dark holes in the sham operated vehicle-injected hippocampal sections represent the normal appearance of neuronal cell bodies. DG: Dentate gyrus. **(B)** Fluorescence image represents abnormal intracellular zinc accumulation after colchicine injection in the hippocampal dentate granule cells. **(C)** The bright white TSQ fluorescence in the cell bodies from the colchicine with CaEDTA-injected hippocampal sections. Zinc chelation did not prevent abnormal zinc accumulation in the dentate granule cells. **(D)** Bar graph depicts the number of TSQ (+) neurons in the DG area. TSQ (+) neurons were counted from vehicle- and colchicine-injected rats at 24 hours later. Fluorescent photomicrographs show Fluoro Jade B (FJB) stained hippocampal dentate granule cells layer **(E,F,G)**. **(E)** The dark holes in the sham operated vehicle-injected hippocampal sections represent the normal appearance of neuronal cell bodies. DG: Dentate gyrus. **(F)** Fluorescence image represents degenerating neurons in the hippocampal dentate granule cells 24 hours after colchicine injection. **(G)** The bright green FJB (+) fluorescence in the cell bodies from the colchicine with CaEDTA-injected hippocampal sections. Zinc chelation did not prevent neuronal degeneration in the dentate granule cells layer. Scale bar in (G) represents 100 μm. **(H)** Bar graph depict the number of FJB (+) neurons in the DG area. FJB (+) neurons were counted from vehicle- and colchicine-injected rats at 24 hours later. Values are presented as means+S.E. Asterisk (*) denotes difference from vehicle-injected rats at $P < 0.05$.

Figure 5. Vincristine-induced intracellular zinc accumulation and neuron death in the dentate granule cell layer of hippocampus.

Fluorescent photomicrographs show TSQ zinc staining in the hippocampal dentate granule cells layer at 24 hours after vincristine injection. **(A)** TSQ fluorescent image represents abnormal intracellular zinc accumulation in the hippocampal dentate granule cells. Green colored neurons in the DG area are TSQ positive neurons. **(B)** Light microscopic images show haematoxylin and eosin (H&E) stained hippocampal sections. Purple colored neurons represent normal, un-injured neurons in the hippocampus. Vincristine injection produces eosinophilic neurons in the dentate granule cell layer. **(C)** Image was enlarged from square box area from (B). Scale bar in (B,C) represents 100 μm.

Figure 6. Proposed colchicine-induced neuron death.

This schematic drawing indicates that colchicine-induced neuron death caused by intracellular zinc accumulation after axonal transport block. **1)** Normal axonal flow. Cytoplasmic and vesicular zinc are normally regulated by axonal flow. **2)** Blocked axonal flow by colchicine. Anterograde and retrograde axonal flow of zinc is prevented by colchicine**. 3)** Zinc accumulation and neuron death. Intracellular free zinc accumulation causes neuron death. ◆ represents proteins. ● represents free zinc. ◆—● represents bound zinc with proteins.

References

1. W. Graham and J. B. Roberts, *Annals of the rheumatic diseases*, 1953, 12, 16-19.

2. E. F. Hartung, *Annals of the rheumatic diseases*, 1954, 13, 190-200.

3. M. J. Ahern, C. Reid, T. P. Gordon, M. McCredie, P. M. Brooks and M. Jones, *Australian and New Zealand journal of medicine*, 1987, 17, 301-304.

4. E. Ben-Chetrit and M. Levy, *Seminars in arthritis and rheumatism*, 1991, 20, 241-246.

5. M. Imazio, M. Bobbio, E. Cecchi, D. Demarie, F. Pomari, M. Moratti, A. Ghisio, R. Belli and R. Trinchero, *Archives of internal medicine*, 2005, 165, 1987-1991.

6. M. Imazio, E. Cecchi, S. Ierna and R. Trinchero, *J Cardiovasc Med (Hagerstown)*, 2007, 8, 613-617.

7. C. Evereklioglu, *Survey of ophthalmology*, 2005, 50, 297-350.

8. D. F. Emerich and T. J. Walsh, *Brain Res*, 1990, 517, 157-167.

9. Y. Nakagawa, S. Nakamura, Y. Kase, T. Noguchi and T. Ishihara, *Brain Res*, 1987, 408, 57-64.

10. R. J. Lasek, *Exp Neurol*, 1968, 21, 41-51.

11. R. B. Goldschmidt and O. Steward, *Proc Natl Acad Sci U S A*, 1980, 77, 3047-3051.

12. R. B. Goldschmidt and O. Steward, *Neuroscience*, 1982, 7, 695-714.

13. G. Danscher and J. O. Rytter Norgaard, *J Histochem Cytochem*, 1985, 33, 706-710.

14. C. J. Frederickson, *Int Rev Neurobiol*, 1989, 31, 145-238.

15. J. Perez-Clausell and G. Danscher, *Brain Res*, 1985, 337, 91-98.

16. S. Y. Assaf and S. H. Chung, *Nature*, 1984, 308, 734-736.

17. G. A. Howell, M. G. Welch and C. J. Frederickson, *Nature*, 1984, 308, 736-738.

18. C. J. Frederickson, M. D. Hernandez, S. A. Goik, J. D. Morton and J. F. McGinty, *Brain Res*, 1988, 446, 383-386.

19. C. J. Frederickson, M. D. Hernandez and J. F. McGinty, *Brain Res*, 1989, 480, 317-321.

20. S. W. Suh, R. B. Thompson and C. J. Frederickson, *Neuroreport*, 2001, 12, 1523-1525.

21. J. Y. Koh, S. W. Suh, B. J. Gwag, Y. Y. He, C. Y. Hsu and D. W. Choi, *Science*, 1996, 272, 1013-1016.

22. J. M. Lee, G. J. Zipfel, K. H. Park, Y. Y. He, C. Y. Hsu and D. W. Choi, *Neuroscience*, 2002, 115, 871-878.

23. S. W. Suh, J. W. Chen, M. Motamedi, B. Bell, K. Listiak, N. F. Pons, G. Danscher and C. J. Frederickson, *Brain Res*, 2000, 852, 268-273.

24. S. W. Suh, C. J. Frederickson and G. Danscher, *J Cereb Blood Flow Metab*, 2006, 26, 161-169.

25. S. W. Suh, P. Garnier, K. Aoyama, Y. Chen and R. A. Swanson, *Neurobiol Dis*, 2004, 16, 538-545.

26. S. W. Suh, A. M. Hamby, E. T. Gum, B. S. Shin, S. J. Won, C. T. Sheline, P. H. Chan and R. A. Swanson, *J Cereb Blood Flow Metab*, 2008, 28, 1697-1706.

27. D. W. Choi and J. Y. Koh, *Annu Rev Neurosci*, 1998, 21, 347-375.

28. J. H. Weiss, S. L. Sensi and J. Y. Koh, *Trends Pharmacol Sci*, 2000, 21, 395-401.

29. S. L. Sensi, P. Paoletti, J. Y. Koh, E. Aizenman, A. I. Bush and M. Hershfinkel, *J Neurosci*, 2011, 31, 16076-16085.

30. Y. H. Kim, E. Y. Kim, B. J. Gwag, S. Sohn and J. Y. Koh, *Neuroscience*, 1999, 89, 175-182.

31. S. L. Sensi, H. Z. Yin, S. G. Carriedo, S. S. Rao and J. H. Weiss, *Proc Natl Acad Sci U S A*, 1999, 96, 2414-2419.

32. C. T. Sheline, M. M. Behrens and D. W. Choi, *J Neurosci*, 2000, 20, 3139-3146.

33. C. T. Sheline, H. Wang, A. L. Cai, V. L. Dawson and D. W. Choi, *Eur J Neurosci*, 2003, 18, 1402-1409.

34. Y. H. Kim and J. Y. Koh, *Exp Neurol*, 2002, 177, 407-418.

35. S. W. Suh, E. T. Gum, A. M. Hamby, P. H. Chan and R. A. Swanson, *J Clin Invest*, 2007, 117, 910-918.

36. Y. H. Ahn, Y. H. Kim, S. H. Hong and J. Y. Koh, *Exp Neurol*, 1998, 154, 47-56.

37. J. Y. Koh, *Molecular neurobiology*, 2001, 24, 99-106.

38. C. J. Frederickson, E. J. Kasarskis, D. Ringo and R. E. Frederickson, *J Neurosci Methods*, 1987, 20, 91-103.

39. S. W. Suh, K. Listiack, B. Bell, J. Chen, M. Motamedi, D. Silva, G. Danscher, W. Whetsell, R. Thompson and C. Frederickson, *J Histochem Cytochem*, 1999, 47, 969-972.

40. L. C. Schmued and K. J. Hopkins, *Brain Res*, 2000, 874, 123-130.

41. S. W. Suh, K. Aoyama, Y. Chen, P. Garnier, Y. Matsumori, E. Gum, J. Liu and R. A. Swanson, *J Neurosci*, 2003, 23, 10681-10690.

42. T. A. Yednock, C. Cannon, L. C. Fritz, F. Sanchez-Madrid, L. Steinman and N. Karin, *Nature*, 1992, 356, 63-66.

43. G. Danscher, G. Howell, J. Perez-Clausell and N. Hertel, *Histochemistry*, 1985, 83, 419-422.

44. G. Danscher and M. Stoltenberg, *J Histochem Cytochem*, 2005, 53, 141-153.

45. S. W. Suh, S. M. Jo, Z. Vajda and G. Danscher, *Neurosci Lett*, 2005, 377, 164-169.

46. G. Danscher, *The Histochemical journal*, 1996, 28, 361-373.

47. S. W. Suh, S. M. Jo, Z. Vajda and G. Danscher, *Brain Res*, 2001, 895, 25-32.

48. R. E. Cull, *Exp Brain Res*, 1975, 24, 97-101.

49. A. Takeda, Y. Kodama, M. Ohnuma and S. Okada, *Brain Res Bull*, 1998, 47, 103-106.

50. T. L. Williamson and D. W. Cleveland, *Nat Neurosci*, 1999, 2, 50-56.

51. T. J. Craddock, J. A. Tuszynski, D. Chopra, N. Casey, L. E. Goldstein, S. R. Hameroff and R. E. Tanzi, *PLoS One*, 2012, 7, e33552.

52. Z. Sahenk and J. R. Mendell, *Brain Res*, 1980, 186, 343-353.

53. M. K. Christensen and C. J. Frederickson, *J Comp Neurol*, 1998, 400, 375-390.

54. Z. Y. Wang and A. Dahlstrom, *Neurochem Res*, 2008, 33, 2472-2479.

55. L. Aniksztejn, G. Charton and Y. Ben-Ari, *Brain Res*, 1987, 404, 58-64.

56. L. Slomianka, G. Danscher and C. J. Frederickson, *Neuroscience*, 1990, 38, 843-854.

Figure 1.

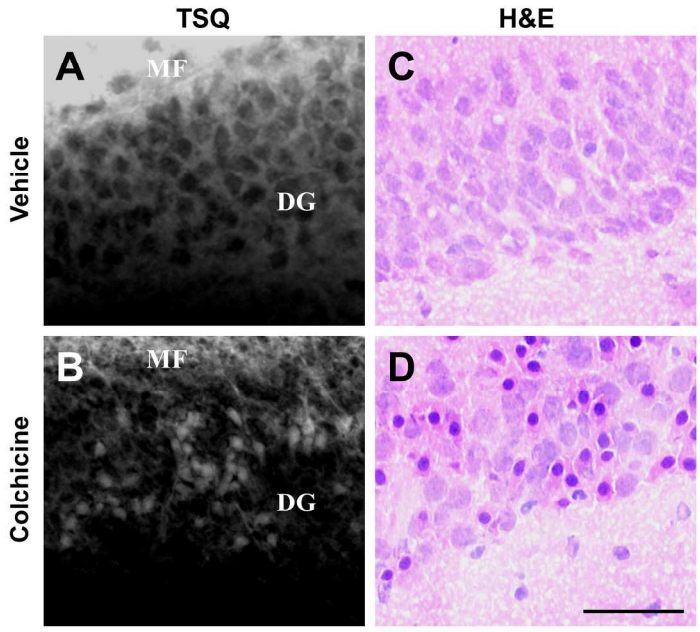

215x287mm (300 x 300 DPI)

Figure 2.

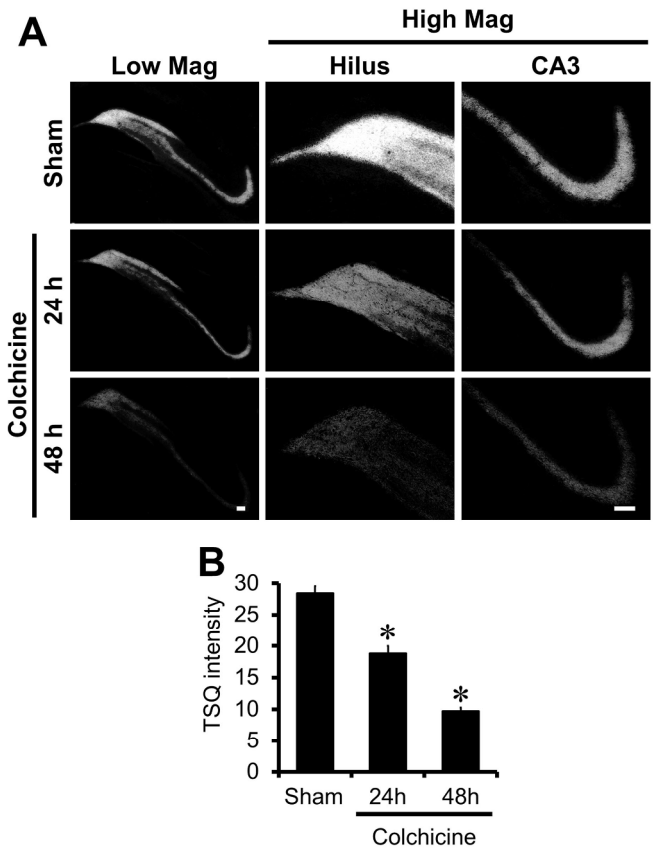

215x287mm (300 x 300 DPI)

Figure 3.

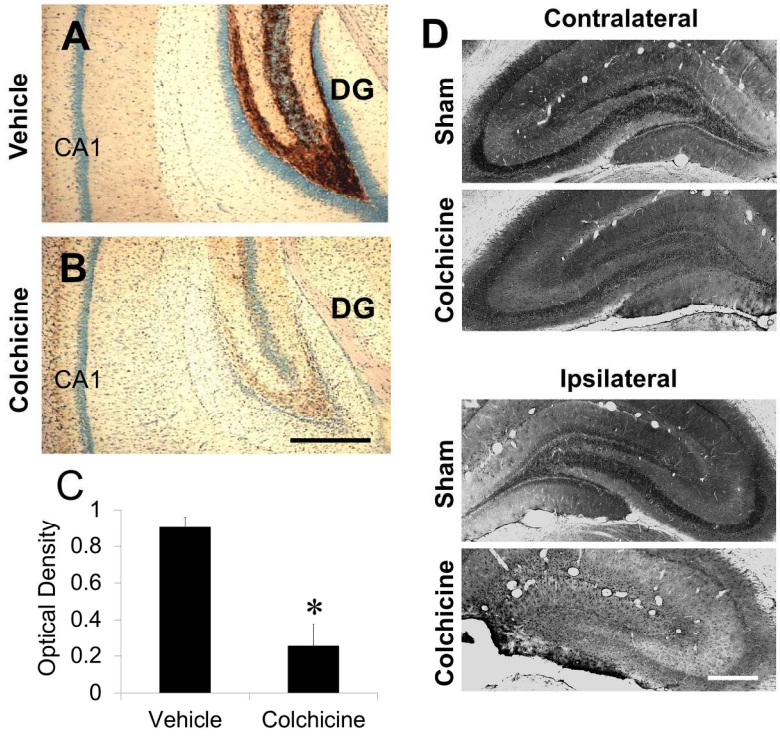

215x287mm (300 x 300 DPI)

Figure 4.

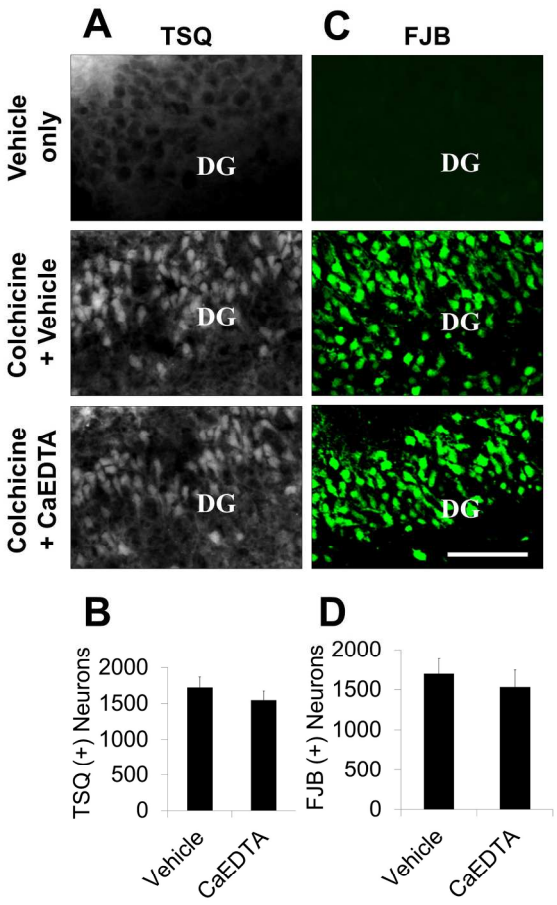

215x287mm (300 x 300 DPI)

Figure 5.

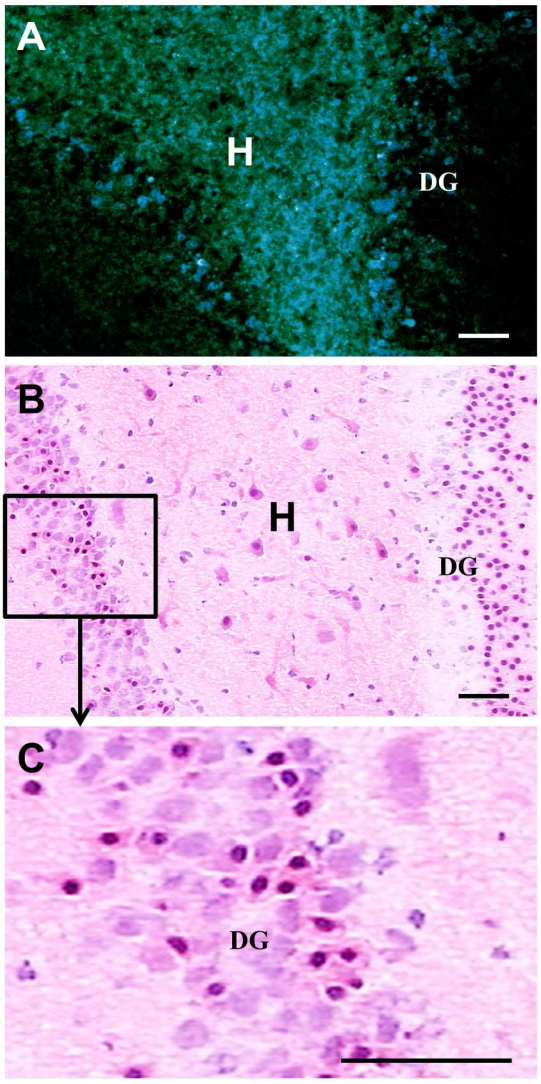

215x287mm (300 x 300 DPI)

Figure 6.

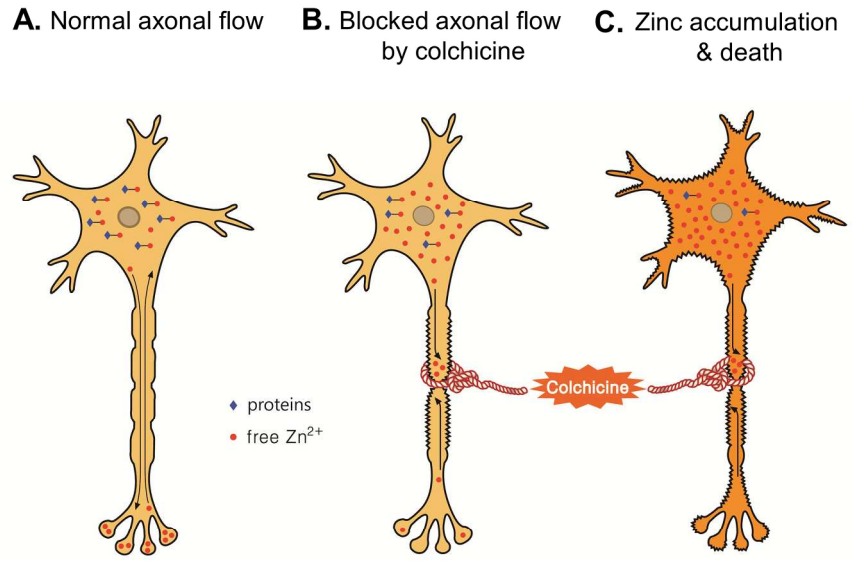

215x287mm (300 x 300 DPI)